Colloidal Polymers with Controlled Sequence and Branching Constructed from Magnetic Field Assembled Nanoparticles

Markus B. Bannwarth,*,†,§,∥ Stefanie Utech,‡ Sandro Ebert,† David A. Weitz,‡ Daniel Crespy,*,† and Katharina Landfester†

†Max Planck Institute for Polymer Research, Ackermannweg 10, 55128 Mainz, Germany, ‡Department of Physics and School of Engineering and Applied Sciences, Harvard University, Cambridge, Massachusetts 02138, United States, §Graduate School of Materials Science in Mainz, Staudinger Weg 9, 55128 Mainz, Germany, and ∥Empa, Laboratory for Protection and Physiology, Lerchenfeldstrasse 5, CH-9014 St. Gallen, Switzerland

ABSTRACT The assembly of nanoparticles into polymer-like architectures is challenging and usually requires highly defined colloidal building blocks. Here, we show that the broad size-distribution of a simple dispersion of magnetic nanocolloids can be exploited to obtain various polymer-like architectures. The particles are assembled under an external magnetic field and permanently linked by thermal sintering. The remarkable variety of polymer—analogue architectures that arises from this simple process ranges from statistical and block copolymer-like sequencing to branched chains and networks. This library of architectures can be realized by controlling the sequencing of the particles and the junction points via a size-dependent self-assembly of the single building blocks.

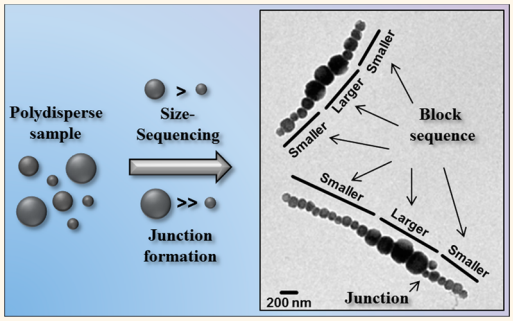

KEYWORDS: magnetic self-assembly · colloidal polymers · controlled sequencing · nanoparticles

In polymer chemistry, a large abundance of elaborate architectures are synthesized from easily accessible and highly defined molecular (monomeric) units. By contrast, the assembly of colloidal building blocks to form polymer-like architectures is usually highly limited by their homogeneity in size, composition, and surface structuring, which provide defined interactions between the colloids. In order to achieve such a directed binding between colloids, large efforts have been made to shape the surface of colloids accordingly.[1,2] When a site specific reactivity is implemented in the colloids, defined colloidal arrangements can be created with astonishing precision.[3] When the colloids possess two or more binding sites, colloidal polymers in analogy to classical polymers can be created.[4] Commonly, a polymer consisting of only one building unit (homopolymer) can vary in average molecular weight and molecular weight distribution. When two or more building units are implemented, a polymer with variable sequencing of the different monomeric units like block copolymers becomes accessible. The introduction of building blocks with more than two binding sites enables branching within the chain.

Several possibilities are known for the assembly of colloidal building blocks in one- (1D), two- (2D), or three-dimensional (3D) fashion through electrostatic interactions,[5−10] magnetic interactions,[11−15] van der Waals forces,[16−18] or DNA-mediated interactions.[3−5] However, a control over the sequence of the arranged colloids or a control over the junction points in the arrangements to mimic polymer architectures remains challenging. There are only few reports dealing with such polymer—analogue architectures from nanocolloids including the assembly of nanoparticles to form block copolymers[18,19] or the introduction of junction points to form branched chains or networks.[20] However, the methods described for the preparation of these colloidal polymers demand high precision

* Address correspondence to bannwarth@mpip-mainz.mpg.de, crespy@mpip-mainz.mpg.de.

Received for review November 17, 2014 and accepted February 19, 2015.

Published online February 19, 2015
10.1021/nn5065327

colloids and the architectures obtained cannot be easily modified. Hence, current efforts focus on the self-assembly of simple colloidal building blocks. Computer simulations have already predicted the possibility to do so.[21] However, the experimental realization has not been demonstrated to date. Once a synthetic pathway for a facile and versatile self-assembly of simple nanocolloids into polymer-like architectures is achieved, future applications, e.g., in photonics,[22−24] electronics,[25] or robotics,[26] can be envisioned. Further, defined sequencing of colloidal chains can lead to colloidal arrangements, which can knot and fold in analogy to proteins, providing the possibility to construct artificial biopolymers from colloidal building blocks.[27]

Here, we demonstrate the versatile assembly of superparamagnetic polystyrene nanoparticles into various architectures. The assembly can be followed by a permanent linkage of the assembled particles by thermal sintering, allowing a detailed investigation of the assemblies. The process used to generate polymer-like chains and smooth fibers from superparamagnetic polystyrene nanoparticles has been reported previously.[28] Furthermore, the reversible linkage of the colloids has been demonstrated.[29] Here, we show the possibility of tailoring the particle's assembly in terms of controlled sequencing of large and small particles within a chain. Additionally, we control the number of colloidal binding partners per particle in order to achieve branching within the chain. By tailoring these two parameters, a library of polymer−analogue architectures including single branched chains and networks can be created. When nanoparticles of a similar size are used, predominantly linear chains are obtained. By implementing nanoparticles with different sizes, the assembly sequence of larger and smaller colloids and the number of colloidal binding partners per particle can be tailored. Control over the sequence of small and large colloids allows for chain structures with rather block-like or rather statistical sequencing of the differently sized particles within the chain. Furthermore, neighboring particles with a large size difference are likely to introduce a junction point within the chain. Integration of many junction points within a chain (by using a nanoparticle dispersion with a broad size distribution) provides the possibility of generating highly branched nanoparticle chains. Additionally, whole cross-linked networks of nanoparticle chains can be created by using highly concentrated dispersions in the process of chain formation.

RESULTS AND DISCUSSION

We use simple polystyrene nanospheres containing a high loading with superparamagnetic iron oxide nanoparticles to form polymer-like nanoparticle chains in a controlled fashion. The hybrid particles need to possess two essential features for a successful chain formation by an assembly and fusion process: A superparamagnetic feature is implemented by encapsulated iron oxide moieties, which provide the possibility of self-assembling the particles upon application of an external magnetic field. Further, a polymeric moiety enables a permanent linkage of neighboring particles by thermal sintering. As model particles comprising these two features, polystyrene nanospheres containing 50−75 wt % of iron oxides (determined from thermogravimetric analysis, TGA) were used. The high loading with iron oxide provides a strong attraction force between the colloid when applying an external field. To achieve an assembly of the colloids into chains, the attraction force between them has to be higher than the thermal energy of the colloids.[30] The average hydrodynamic diameter (d_h) of the colloids was 80−350 nm (as determined from dynamic light scattering, DLS measurements). The size and polydispersity of the nanoparticles dispersion can be tailored by centrifugation as a size-separation method (see methods for details). The iron oxide is distributed predominantly homogeneous within the particles (Figure S3). In some cases there is a slight polystyrene enrichment on one side of the particles. However, this enrichment does not affect the assembly except for a slight tendency of the particles to form linear zigzag arrangements.[28] Further, the particles possess a zeta potential of −40 to −60 mV, which derives mainly from the covalently bonded comonomer (sodium 4-styrenesulfonate) and self-stabilizes the nanoparticles in the dispersion. Because of the high negative surface charge, the particles repel each other. When however an external magnetic field is applied, the attractive magnetic force between two superparamagnetic particles can be high enough to overcome the energetic barrier created by the negative zeta potential. Thus, the particles can be assembled and subsequently fused in the presence of an external magnetic field resulting in various architectures with polymer resemblance. Without the fusion, the superparamagnetic nanoparticles would disassemble when removing the external field. Thus, a permanent linkage is required to maintain the arrangement permanently. The components of the setup used to achieve this assembly and fusion are depicted in Figure S1. Briefly, a syringe pump is used to insert the nanoparticle dispersion into a tube, which guides the dispersion through a heated oil bath and toward a static ring magnet. Approaching the ring magnet, the dispersion of superparamagnetic nanoparticles starts to feel the external magnetic field of the permanent magnet. Hence, a magnetic dipole is induced in the superparamagnetic particles causing an attractive force between the particles and thus the controlled assembly into one-dimensional chains. After assembly, neighboring particles are fused together under the increased temperatures in the oil bath (for details see methods).

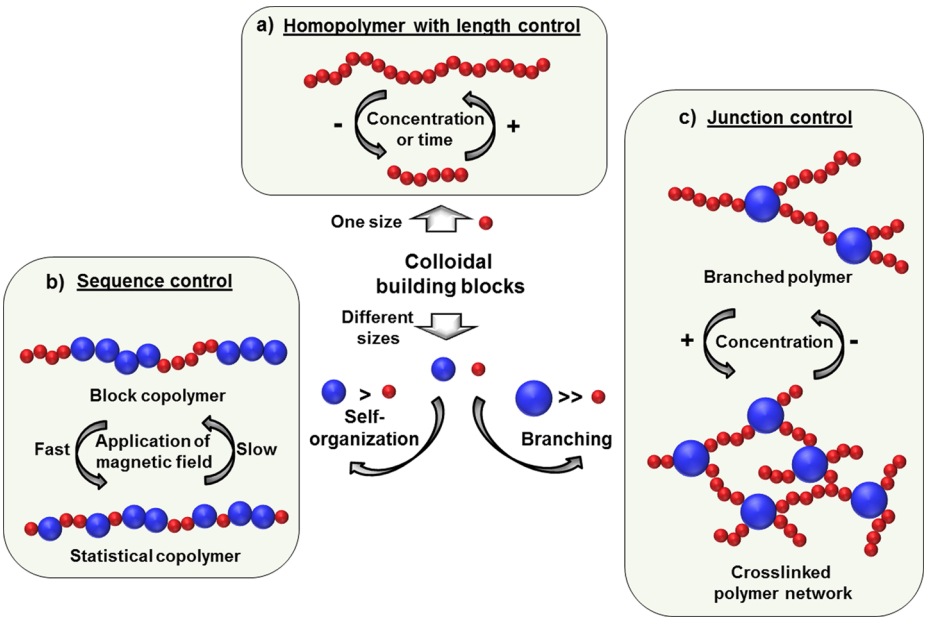

Figure 1. Schematic illustration showing different polymer-like architectures that can be created by a controlled assembly and fusion of superparamagnetic polystyrene nanoparticles. (a) Insertion of a monodisperse nanoparticle dispersion yields predominantly linear nanochains. Depending on the concentration of the nanoparticle dispersion (and the growth time), longer or shorter chains can be obtained. (b) In the case of a polydisperse sample, the different sized particles (colored in red and blue representing small and large particles, respectively) can self-organize into blocks of larger and smaller particles, resulting in colloidal block copolymers or in rather statistical fashion. A slow increase of the external magnetic field assembles the particles in a rather block-like pattern, a fast increase in a rather statistical fashion. (c) The insertion of particles with even larger size differences enables the introduction of junction points. Here, more than two small nanoparticles assemble around a large particle creating a junction point within the nanoparticle chain. By increasing the concentrations of nanoparticles in the dispersion, networks of cross-linked chains can be obtained.

When a dispersion of nanocolloids with a relatively narrow size distribution is used in the process, predominantly linear chains of the nanocolloids are observed (Figure 1a). The length of the chains can be tuned either by the concentration of the nanoparticle dispersion (higher concentration ≙ longer chains) or by the growth time of the chains (longer growth time ≙ longer chains). Use of nanoparticle dispersions with a larger size distribution allows the size-sequencing of larger and smaller particles within a nanoparticle chain. Depending on the assembly conditions, the sequence can be rather statistical or block-like. The assembly conditions can be controlled by the flow rate of the nanoparticle dispersion toward the permanent magnet. The particles approach the permanent magnet fast for high flow rates. Thus, the external field increases rapidly (Figure S2). The rapid increase in external field leads to a rather chaotic assembly of the particles in statistical fashion. On the contrary, a slow flow rate leads to a slow increase in magnetic field and an ordered assembly of the particles by size. Hence, the flow rate and concomitant velocity of external magnetic field application is the key parameter for a variable sequencing of larger and smaller particles within the chain, from preferably statistical to block-like structures (Figure 1b). Furthermore, when the size difference of neighboring nanocolloids is very large, the introduction of junction points is achieved (Figure 1c). The larger the size difference between the particles, the more likely is the creation of such a junction point. By varying the concentration of dispersions containing very large and very small colloids (with a broad size distribution), single branched chains or whole networks of nanoparticle chains can be obtained depending on the concentration of the dispersion. At low concentrations single-branched chains are obtained while higher nanoparticle concentrations typically result in network architectures.

Linear Chains with Size-Sequence Control. Using a dispersion of single nanoparticle building blocks, one-dimensional structures can be governed by the controlled assembly of the nanospheres in the presence of an external magnetic field and permanent linkage of the assembly by physical interactions,[31] encapsulation,[32−34] electrolyte complexes,[35,36] or covalent binding.[37] Here, we use thermal sintering for the fusion of neighboring nanoparticles since the particles are easily accessible and can be produced with various morphologies and the fusion takes place rapidly.[28] Making use of this assembly and fusion process, we found that implementation of nanoparticles with a rather narrow size distribution (preferably $\sigma < 10\%$) yields predominantly linear chains (see Figure S3b for particle characterization and Figure S4 for linear

chains). The length of the chains can be tailored by the concentration of the nanoparticle dispersion and the time the particles have to assemble and fuse. With increasing concentration and time, the length of the chain can be increased.

A closer look at the role of the inserted nanoparticles during the assembly process revealed that the polydispersity of the nanoparticles in dispersion plays a very crucial role for the assembly process and thus the structure of the resulting chain. A nanoparticle dispersion with a rather monodisperse size distribution typically leads to linear chain (in analogy to homopolymers), while a polydisperse size distribution results in the formation of more elaborate structures. Hence, a nanoparticle dispersion with a larger polydispersity can be used to purposely create defined assembly architectures of nanoparticle building blocks. When considering nanoparticles with different sizes (e.g., from a polydisperse sample) as different types of monomers, a sequencing analogous to that known from polymer chemistry can be observed for the assembly of the superparamagnetic polystyrene nanoparticles. Depending on the assembly conditions, block- or statistical copolymer-like sequencing of nanoparticles with different sizes can be observed. The flow parameter provides the basis to control the sequence of differently sized particles within a chain. By tailoring the flow rate of the dispersion toward the permanent magnet, the increase of the magnetic field strength can be controlled (see Figure S1 for flow setup to obtain nanoparticle chains and Figure S2 for distance-dependent magnetic field). Hence, for a faster flow rate of the dispersion toward the permanent magnet, the external magnetic field increases faster. A fast flow rate (fast increase in external magnetic field) leads to a rather statistical sequencing of differently sized particles within the chain. In the case of a slow flow rate (slow increase in external magnetic field), a sequence with smaller and larger particles arranged in size-separated blocks is observed. Hence, the assembly velocity of nanoparticles has to be dependent on how fast the external magnetic field is applied (Figure 2a). Once the particles assemble under the external magnetic field and get in contact with each other, a fast fusion within seconds[28] guarantees to "freeze" the assembled state of the nanoparticles and thus allows for a detailed investigation of the assembly process via TEM imaging (Figure 2b–e).

TEM analysis of nanoparticle chains formed by the controlled assembly and fusion of a nanoparticle dispersion with a rather broad polydispersity (Figure S3a) reveal the possibility of size-self-assembly of nanoparticles to form blocks of similarly sized neighboring particles (Figure 2b,c). Therefore, a slow flow rate of the nanoparticle dispersion toward the permanent magnet should be chosen (~1.5–3 mm·s^{-1} or ~2–4 mL·h^{-1}). Under these conditions, a remarkable

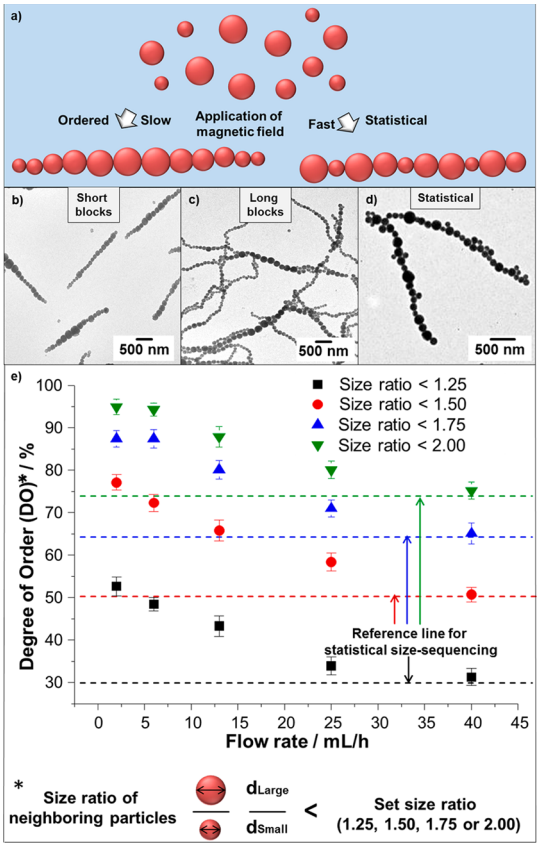

Figure 2. Controlled size-self-assembly of large and small nanoparticles within a chain. (a) Schematics depicting the two possibilities to align a polydisperse sample of nanoparticles. When all particles have the same reactivity, a statistical assembly occurs. In the case of low flow rates (slow increase of the magnetic field), larger particles exhibit a higher reactivity in the early stage of the assembly process (the magnetic field is still relatively low) due to their higher magnetic content and thus their stronger response to the magnetic field. Smaller particles start to assemble later in the process (when the magnetic field strength is increased). Consequently, the larger particles assemble first followed by the assembly of smaller particles at the edges of the chain. In the case of faster flow rates, this size-dependent assembly cannot be observed since the magnetic field increase is too fast to allow for a separated assembly of large particles. Here, smaller and larger particles assemble simultaneously leading to a rather statistical size-sequencing within the chain. (b) TEM image of shorter chains of nanoparticles with the tendency to form small blocks of larger and smaller particles. Often the larger particles are found toward the middle of the chains and the smaller ones toward the ends. (c) TEM image of larger chains with large blocks of larger and smaller particles. (d) TEM image of statistically assembled nanoparticles into chains. (e) Graph illustrating the probability that neighboring particles have similar sizes with respect to the flow conditions. For a slow flow rate, the DO is high and decreases with increasing flow rate.

separation between the larger particles (~200–300 nm) and the smaller particles (~100–150 nm) within the chains can be observed. The size-separation is observed independently of the length of the chains (for lower and higher solid content nanoparticle dispersions, 0.4 and 1.5 wt %, respectively) as shown in Figure 2b,c for short and long chains, respectively. In long chains, however (Figure 2c), long blocks of large or

small particles are possible. In the case of shorter chains (Figure 2b), only short blocks of large or small particles are formed. A rather statistical distribution of larger and smaller particles within the chain is instead observed when a fast flow rate of ~30 mm·s^{-1} or ~40 mL·h^{-1} is applied (Figure 2d). To investigate the difference in size-sequencing with the flow rate, a quantitative analysis was performed. The degree of order (size difference of neighboring particles) was analyzed with respect to the flow rate of the nanoparticle dispersion (see Figure 2e) and therefore with the velocity of the increase of the external magnetic field. The size ratio of neighboring nanoparticles was analyzed and the degree of order (DO) plotted against the flow rate (see Figure 2e for definition of DO). The DO describes the percentage of neighboring particles that have a similar size (<than the set size ratio of 1.25, 1.50, 1.75, or 2.0) as described in Figure 2e. The DO was calculated for a completely statistical arrangement of the nanoparticles with the given size distribution (Figure S3a) and the values added as dashed lines. When the flow rate is increased, the DO of all investigated samples converges toward the dashed line of the statistical arrangement. However, the DO is considerably higher when the flow rate is very slow. Impressively, the probability for neighboring particles to have a size ratio of two or more is significantly higher (5−6 times) for a fast flow rate than for a slow flow rate.

We next direct our attention toward the size-dependent assembly of the colloids with respect to the flow rate and thus the velocity of magnetic field application. Considering that all of the hybrid nanoparticles, no matter how large they are, consist to the same percentage of inorganic iron oxide (as suggested by TGA measurements and TEM analysis), the saturation magnetization of the particles increases linearly with their volume. Thus, the amount of superparamagnetic iron oxides is proportional to the diameter of the particles to a power of three. The pronounced dependence of the nanoparticle size on the iron oxide content and therefore the generated magnetic field of each particle is a key factor in their size-dependent self-assembly. The assembly time τ of the superparamagnetic nanoparticles is (among other factors) dependent on the radius r of the particles and the magnetic field H and can be described in a simplified way as follows:[38,39]

$$\tau \approx \frac{1}{r^6 H^2} \quad (1)$$

Hence, the assembly time is highly dependent on the radius of the nanoparticles. In consequence, one can expect larger particles to assemble faster and smaller particles to assemble later.

In addition to the faster assembly time, the stronger force between larger particles can also lead to a size-dependent assembly. The force F between two particles can be described as follows (for parallel aligned dipoles):[40]

$$F \approx r^6 H^2 \quad (2)$$

Chaining of particles is only possible when the attraction force between two particles is higher than their thermal energy.[30] Hence, for weaker magnetic fields only large particles fulfill this criterion and can chain.

In summary, the strong size-dependency of the assembly time and with the interaction force of magnetic colloids is responsible for their distinct assembly by size within a chain. The size-dependent assembly from an originally polydisperse colloid dispersion is observed, when the magnetic field is ramped-up slowly when applying a slow flow (Figure S2).

However, the size-dependent assembly can be repressed when the magnetic field is ramped-up rapidly. In this case, H reaches a high value very fast. Hence, the attraction force between particles increases fast and the assembly time is accelerated. As a result of the stronger forces between the particles, also smaller particles chain early in the process since their attraction force is stronger than their thermal energy. Further, the accelerated assembly leads to a smaller (average) time difference for the assembly of particles with different radii. Hence, the radius does not play such a dominant role any more.

Because larger particles assembly first (when the field is ramped slowly), one can often observe larger particles in the middle of the chain, whereas the outer parts of the chain are often composed of smaller particles (see Figure 2b and Figure S5). The ordered sequence does not occur in all of the chains. Nevertheless, it is clearly the predominant arrangement. This preferred arrangement of larger particles in the middle of the chain and the smaller particles at the end of the chain additionally underpins the hypothesis for a faster assembly of larger particles when the external magnetic field is applied slowly. Then the smaller particles assemble from both sides of the growing chain. In the case of faster flow rates and thus a fast increase in the magnetic field, a more statistical assembly is obtained. The increase in the magnetic field is too fast for a size-selective assembly of the large particles. The particle dispersion is directly exposed to a rather strong magnetic field, which results in the statistical assembly of small and large particles.

In conclusion, the sequence of larger and smaller particles within a nanochain can be controlled by the flow rate and thus by the ramping of the magnetic field. Owing to this simple relationship, the formation of a statistical or a block-like distribution of different particle sizes within a chain is controllable by the flow rate of the dispersion in the device.

Formation of Single Branched Chains or Networks of Chains. When the number of binding partners of a building

block in a polymer is higher than two, a junction is formed. At a certain concentration and number of junction points, networks can be created.[41] When colloids at a certain concentration interact with each other they can form all different types of 3D structures from gel to crystals and glasses with abundant uses.[42,43] In these cases, the interactions between the colloids are usually not site specific. Implementation of site-specificity into colloids is challenging. To prepare (nano)colloids with a defined number of binding partners, a certain anisotropy is usually introduced on the surface of the particles. This can either be an anisotropy in shape as in the case of buckling[44] or faceting,[45] or an anisotropy in the surface functionalization[46,47] or roughness.[47,48] Then, the defined anisotropy can be used to selectively link (nano)particles in many different ways.[49]

Here, we show that the surface of the colloids does not have to be specifically designed in order to achieve a binding of more than two colloids to one building block. Conversely, the size ratio of two neighboring particles is used to introduce junction points into the linear arrangement of the hybrid nanoparticles induced by the magnetic field. The formation of a junction point where three or more small colloids binding to one large particle is schematically depicted in Figure 3a. The combination of a large particle with several small binding partners provides the basis for such a junction. The reason for the high probability to form junctions when the size ratio of neighboring particles is large originates mainly from steric considerations: The larger the size ratio of two particles, the more small particles "fit" next to a large particle. The occurrence of junctions as a function of the large to small ratio of neighboring particles was analyzed by TEM measurements and quantified as shown in Figure 3e (see methods for details). For neighboring particles with similar sizes, almost no junctions were observed. However, when increasing the size ratio between neighboring particles, the probability to obtain a junction point increases significantly with the size ratio of the two neighboring particles. Two examples for a junction are shown as TEM images in Figure 3b,c. The first image shows three small colloids binding to one large particle, and the second image shows four small colloids in neighboring position to one large building block. As a result, junctions are introduced in the nanoparticle chains.

The influence of the flow rate on the sequence of large and small particles within the chain has already been discussed. With increasing flow rate, neighboring particles tend to arrange in a statistical fashion and do not self-assemble by size. To obtain junction points, a rather statistical sequencing of larger and smaller particles promotes a higher probability to obtain junction points. The dependence of the probability of obtaining junction points was quantified with respect

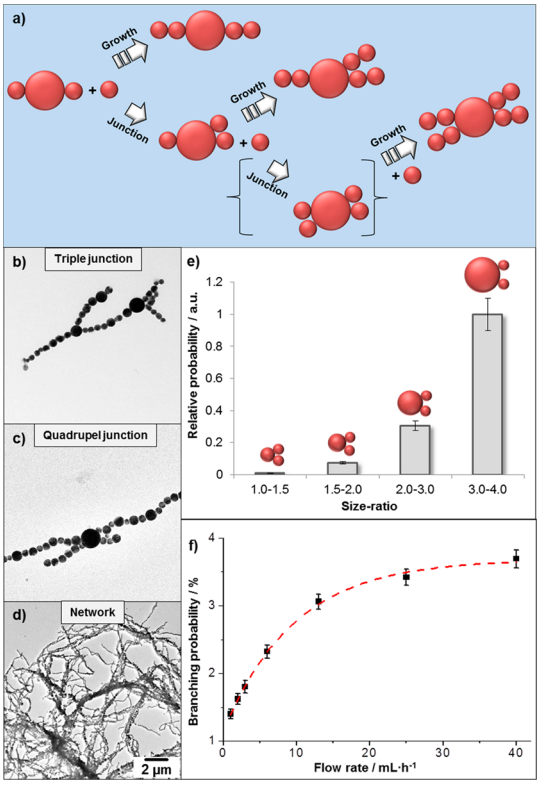

Figure 3. Introduction of junction points into a growing chain of nanoparticles. (a) Schematic illustration of the two possibilities of a growing chain. When particles of a similar size "react" with each other, linear growth commonly occurs. When two small particles meet a very large particle, the introduction of a junction becomes likely. (b) TEM image of a branched nanoparticles chain where the larger particles act as junction point. (c) TEM image of a branched chain with a very large particle acting as junction point in both directions of the chain. (d) TEM image of a whole network of cross-linked nanoparticle chains by a combination of large chains with high branching probability (a nanoparticle dispersion with high polydispersity). (e) Graph illustrating the relative probability for the occurrence of junction points with the size ratio of two neighboring particles. Larger size ratios between small and large particles increase the likelihood of branching to occur. In the case of smaller ratios, mainly linear chains result. (f) Dependence of the percentage of branching points in a nanoparticle chain with the flow speed.

to the flow rate of the particle dispersion as shown in Figure 3f. The quantification clearly underlines the relationship between particle flow rate and branching probability. Thus, the introduction of junction points within the chain can be tailored not only by the size difference (polydispersity) of neighboring particles but additionally by the flow conditions.

It is also possible to form a network of nanoparticle chains (Figure 3d). The occurrence of a network can be easily calculated based on the probability of a junction point per particle and the amount of particles per chain, the degree of polymerization. The critical extent for the formation of a network is reached when the number of junction points equals the inverse of the degree of polymerization.[50] From this relationship, the formation of a network can be easily calculated and

predicted. On the basis of the possibility to tune the chain length with time and concentration in addition to introduce junction points by controlling the flow rate and polydispersity, networks of nanoparticles can be created with the process described.

CONCLUSIONS

A novel method for the fabrication of various polymer-like architectures from nanocolloids using a facile assembly and fusion principle was demonstrated. The size difference/polydispersity of the inserted colloids can thereby be utilized to create a library of different architectures. Linear chains can be obtained from nanoparticle dispersions with a rather narrow size distribution. For dispersions with higher polydispersity, the sequence of larger and smaller particles within the chain can be controlled by the applied flow rate and thus by the velocity of the magnetic field application. Because of this simple relationship, the formation of block-like or statistical copolymers can be well controlled. Furthermore, junction points can be introduced into the chains and can be tailored by the flow conditions and the polydispersity of the sample. Introduction of single junction points into chains as well as the fabrication of whole networks of particles becomes possible. Thus, highly elaborate architectures can be created from dispersions with low precision colloids. In summary, an innovative method for the generation of complex yet defined architectures by magnetic assembly and thermal fusion is demonstrated, which can provide a means to make defined structures from simple spherical building blocks.

METHODS

Synthesis of Iron Oxide Nanoparticles. Oleate-capped iron oxide nanoparticles were synthesized after a reported procedure with slight modifications.[28,51] Briefly, 12.0 g of ferrous chloride tetrahydrate and 24.4 g of ferric chloride hexahydrate were dissolved in 100 mL of deionized water at room temperature and filtered to remove insoluble impurities. Subsequently, 40 mL of a 28% ammonium hydroxide solution was added dropwise followed by the addition of 4.0 g of oleic acid. The reaction mixture was heated to 70 °C for 1 h and afterward to 110 °C for 2 h. The evaporating water was constantly refilled with deionized water. Within the heating step, clustering and precipitation of the iron oxide nanoparticles was observed. After cooling the reaction mixture, the resulting black residue was rinsed several times with deionized water followed by drying under vacuum at 40 °C overnight.

Synthesis of Polystyrene Nanoparticles with Encapsulated Iron Oxide. The synthesis of polystyrene nanoparticles with encapsulated iron oxide was performed as described previously.[28,52] Briefly, 1 g of oleate-capped iron oxide nanoparticles was redispersed in 2 g of *n*-octane for 30 min in a sonication bath followed by the addition of 24 g of an aqueous solution containing 25 mg of sodium dodecyl sulfate (SDS). The two phase system was sonified with a tip sonifier for 3 min under ice cooling (70% amplitude, 10 s pulse, 5 s pause) and stirred nonmagnetically (KPG-stirrer) at room temperature. Separately, 1 g of styrene was mixed with 30 mg of *n*-hexadecane and 24 g of 10 mg of SDS containing aqueous solution. After sonication with a tip sonifier for 1 min under ice cooling (10% amplitude, 5 s pulse, 5 s pause), the dispersion was added to the iron oxide containing dispersion. Nitrogen was bubbled through the combined dispersions for 5 min, 20 mg of potassium persulfate (KPS) and 30 mg of sodium styrenesulfonate were added, and the reaction mixture was heated to 80 °C under stirring for 8 h. Purification of the superparamagnetic polystyrene particles was carried out magnetically and by centrifugation. The obtained nanoparticles were analyzed via DLS (Nicomp zetasizer at a fixed angle of 90° at 25 °C), TGA (thermobalance Mettler Toledo TGA/SDTA 851 at a heating rate of 10 $K \cdot min^{-1}$ from 25−800 °C under nitrogen atmosphere), zeta potential measurements (Malvern Instruments Zeta Nanosizer at a detection angle of 173° in an excess of 10^{-3} M KCl aqueous solution), by solid content determination (gravimetrically), and TEM imaging (Zeiss EM912 at an acceleration voltage of 120 kV on 300-mesh carbon-coated copper grid.). To lower the particle size distribution, the particles were separated by size by centrifugation for 15 min at revolutions per minute between 600 and 1600.

Linear Assembly and Fusion of Superparamagnetic Polymer Hybrid Nanoparticles. The setup shown in Figure S1 was used for chain formation from iron oxide/polymer hybrid nanoparticles. For long linear chains (≥40 nanoparticles per chain), the polydispersity of the nanoparticle dispersion should be narrow (σ < 10%). Therefore, an aqueous nanoparticle dispersion (0.2−2 wt % solid content) containing 0.05 wt % SDS was pumped through a glass (or silicone) tube (approximately 0.7 mm in diameter) with a flow rate of 1−40 $mL \cdot h^{-1}$ (Postnova analytics PN 1610 syringe closing system). The middle part of the tube was positioned in a heated oil bath (at ∼95 °C) with a static ring magnet (>300 mT closest to the magnet) in the middle. When nanoparticle dispersions with a higher polydispersity are used, also predominantly linear chains can be obtained. Therefore, the flow rate should be slow (1−5 $mL \cdot h^{-1}$). Once pumped through the system, the chains can be collected at the end of the tube. For TEM analysis, the chains were precipitated magnetically and redispersed in deionized water to remove excess SDS. For determination of the average number of particles per chain, 100 chains were analyzed per sample.

Control over Self-Assembly by Particle Sizes to Form Block Copolymers. To obtain nanoparticle chains with a controlled sequence, a dispersion with broader size distribution (typically 30% ≤ σ ≤ 40%) was implemented in the process described above for chain formation. The sequence of the resulting chain in terms of neighboring nanoparticle sizes can be controlled by the flow conditions (as shown in Figure 2e). Analysis of the chains was done from TEM images. Determination of the particle diameter was done using ImageJ. For the determination of the degree of order, >500 particles were counted from TEM images.

Introducing Junction Points to Control the Degree of Branching and Form Networks. Chains containing junction points can be made using the same process. Here, the polydispersity of the nanoparticle dispersion should be high in order to form many junction points ($\sigma \approx 50\%$). Different flow speeds were investigated (1−40 $mL \cdot h^{-1}$) to determine the influence of the flow rate on the branching probability (Figure 3f). Analysis was done from TEM images using ImageJ to calculate the particle diameters. For the study of the branching probability with respect to the size ratio of neighboring particles, 300 junction points were analyzed from TEM images. The junction points were categorized into different size-ratio regimes (size-ratio of 1.0−1.5; 1.5−2.0; 2.0−3.0; 3.0−4.0) and the number of junction points that were counted from TEM images for each of the regimes divided by the probability that two neighboring nanoparticles meet this size-ratio criterion in a statistical chain.

Conflict of Interest: The authors declare no competing financial interest.

Supporting Information Available: TEM images size distribution data of single nanoparticles. TEM images of nanoparticle chains and coloration of the TEM images to show block

formation and branching. Description of the coloration process of TEM images from nanoparticle chains with differently sized particles. Instrumental setup for the assembly and fusion of nanoparticles under magnetic field and temperature increase. Calculation of the statistical size-variation of neighboring nanoparticles. Magnetic field strength with distance to the magnet. This material is available free of charge via the Internet at http://pubs.acs.org.

Acknowledgment. The authors thank Dr. R. Muñoz-Espí and G. Sanchez for assistance with setting up the device for nanoparticle assembly and fusion. M.B.B. gratefully acknowledges financial support by the Excellence Initiative (DFG/GSC 266). S.U. was financially supported by the Deutsche Forschungsgemeinschaft. This work was supported by the NSF (DMR-1310266) and the Harvard Materials Research Science and Engineering Center (DMR-0820484). J. Cui, S. W. Kazer, and S. Ulrich are acknowledged for experimental support.

REFERENCES AND NOTES

1. Sacanna, S.; Korpics, M.; Rodriguez, K.; Colón-Meléndez, L.; Kim, S.-H.; Pine, D. J.; Yi, G.-R. Shaping Colloids for Self-Assembly. *Nat. Commun.* **2013**, *4*, 1688.
2. Stevens, M. J. How Shape Affects Microtubule and Nanoparticle Assembly. *Science* **2014**, *343*, 981–982.
3. Wang, Y. F.; Wang, Y.; Breed, D. R.; Manoharan, V. N.; Feng, L.; Hollingsworth, A. D.; Weck, M.; Pine, D. J. Colloids with Valence and Specific Directional Bonding. *Nature* **2012**, *491*, 51–55.
4. Grzelczak, M.; Vermant, J.; Furst, E. M.; Liz-Marzan, L. M. Directed Self-Assembly of Nanoparticles. *ACS Nano* **2010**, *4*, 3591–3605.
5. Fukino, T.; Joo, H.; Hisada, Y.; Obana, M.; Yamagishi, H.; Hikima, T.; Takata, M.; Fujita, N.; Aida, T. Manipulation of Discrete Nanostructures by Selective Modulation of Noncovalent Forces. *Science* **2014**, *344*, 499–504.
6. Bharti, B.; Findenegg, G. H.; Velev, O. D. Co-Assembly of Oppositely Charged Particles into Linear Clusters and Chains of Controllable Length. *Sci. Rep.* **2012**, *2*, 1–4.
7. Warner, M. G.; Hutchison, J. E. Linear Assemblies of Nanoparticles Electrostatically Organized on DNA Scaffolds. *Nat. Mater.* **2003**, *2*, 272–277.
8. Li, F.; Josephson, D. P.; Stein, A. Colloidal Assembly: The Road from Particles to Colloidal Molecules and Crystals. *Angew. Chem., Int. Ed.* **2011**, *50*, 360–388.
9. Bannwarth, M.; Crespy, D. Combining the Best of Two Worlds: Nanoparticles and Nanofibers. *Chem.—Asian J.* **2014**, *9*, 2030–2035.
10. Vutukuri, H. R.; Demirors, A. F.; Peng, B.; van Oostrum, P. D. J.; Imhof, A.; van Blaaderen, A. Colloidal Analogues of Charged and Uncharged Polymer Chains with Tunable Stiffness. *Angew. Chem., Int. Ed.* **2012**, *51*, 11249–11253.
11. Yavuz, C. T.; Mayo, J. T.; Yu, W. W.; Prakash, A.; Falkner, J. C.; Yean, S.; Cong, L. L.; Shipley, H. J.; Kan, A.; Tomson, M.; Natelson, D.; Colvin, V. L. Low-Field Magnetic Separation of Monodisperse Fe3O4 Nanocrystals. *Science* **2006**, *314*, 964–967.
12. Yang, Y.; Gao, L.; Lopez, G. P.; Yellen, B. B. Tunable Assembly of Colloidal Crystal Alloys Using Magnetic Nanoparticle Fluids. *ACS Nano* **2013**, *7*, 2705–2716.
13. Demirors, A. F.; Pillai, P. P.; Kowalczyk, B.; Grzybowski, B. A. Colloidal Assembly Directed by Virtual Magnetic Moulds. *Nature* **2013**, *503*, 99–103.
14. Majetich, S. A.; Wen, T.; Booth, R. A. Functional Magnetic Nanoparticle Assemblies: Formation, Collective Behavior, and Future Directions. *ACS Nano* **2011**, *5*, 6081–6084.
15. Hill, L. J.; Richey, N. E.; Sung, Y.; Dirlam, P. T.; Griebel, J. J.; Lavoie-Higgins, E.; Shim, I.-B.; Pinna, N.; Willinger, M.-G.; Vogel, W.; Benkoski, J. J.; Char, K.; Pyun, J. Colloidal Polymers from Dipolar Assembly of Cobalt-Tipped CdSe@CdS Nanorods. *ACS Nano* **2014**, *8*, 3272–3284.
16. Min, Y.; Akbulut, M.; Kristiansen, K.; Golan, Y.; Israelachvili, J. The Role of Interparticle and External Forces in Nanoparticle Assembly. *Nat. Mater.* **2008**, *7*, 527–538.
17. Liu, K.; Nie, Z. H.; Zhao, N. N.; Li, W.; Rubinstein, M.; Kumacheva, E. Step-Growth Polymerization of Inorganic Nanoparticles. *Science* **2010**, *329*, 197–200.
18. Groschel, A. H.; Walther, A.; Lobling, T. I.; Schacher, F. H.; Schmalz, H.; Muller, A. H. E. Guided Hierarchical Co-Assembly of Soft Patchy Nanoparticles. *Nature* **2013**, *503*, 247–251.
19. Liu, K.; Lukach, A.; Sugikawa, K.; Chung, S.; Vickery, J.; Therien-Aubin, H.; Yang, B.; Rubinstein, M.; Kumacheva, E. Copolymerization of Metal Nanoparticles: A Route to Colloidal Plasmonic Copolymers. *Angew. Chem.* **2014**, *126*, 2686–2691.
20. Demortière, A.; Snezhko, A.; Sapozhnikov, M. V.; Becker, N.; Proslier, T.; Aranson, I. S. Self-Assembled Tunable Networks of Sticky Colloidal Particles. *Nat. Commun.* **2014**, *5*, 3117.
21. Grünwald, M.; Geissler, P. L. Patterns without Patches: Hierarchical Self-Assembly of Complex Structures from Simple Building Blocks. *ACS Nano* **2014**, *8*, 5891–5897.
22. Benson, O. Assembly of Hybrid Photonic Architectures from Nanophotonic Constituents. *Nature* **2011**, *480*, 193–199.
23. He, L.; Wang, M.; Ge, J.; Yin, Y. Magnetic Assembly Route to Colloidal Responsive Photonic Nanostructures. *Acc. Chem. Res.* **2012**, *45*, 1431–1440.
24. Klinkova, A.; Choueiri, R. M.; Kumacheva, E. Self-Assembled Plasmonic Nanostructures. *Chem. Soc. Rev.* **2014**, *43*, 3976–3991.
25. Wang, L.; Xu, L.; Kuang, H.; Xu, C.; Kotov, N. A. Dynamic Nanoparticle Assemblies. *Acc. Chem. Res.* **2012**, *45*, 1916–1926.
26. Snezhko, A.; Aranson, I. S. Magnetic Manipulation of Self-Assembled Colloidal Asters. *Nat. Mater.* **2011**, *10*, 698–703.
27. Coluzza, I.; van Oostrum, P. D. J.; Capone, B.; Reimhult, E.; Dellago, C. Sequence Controlled Self-Knotting Colloidal Patchy Polymer. *Phys. Rev. Lett.* **2013**, *110*, 075501.
28. Bannwarth, M. B.; Kazer, S. W.; Ulrich, S.; Glasser, G.; Crespy, D.; Landfester, K. Well-Defined Nanofibers with Tunable Morphology from Spherical Colloidal Building Blocks. *Angew. Chem., Int. Ed.* **2013**, *52*, 10107–10111.
29. Bannwarth, M. B.; Weidner, T.; Eidmann, E.; Landfester, K.; Crespy, D. Reversible Redox-Responsive Assembly/Disassembly of Nanoparticles Mediated by Metal Complex Formation. *Chem. Mater.* **2014**, *26*, 1300–1302.
30. Bharti, B.; Findenegg, G. H.; Velev, O. D. Analysis of the Field-Assisted Permanent Assembly of Oppositely Charged Particles. *Langmuir* **2014**, *30*, 6577–6587.
31. Khalil, K. S.; Sagastegui, A.; Li, Y.; Tahir, M. A.; Socolar, J. E. S.; Wiley, B. J.; Yellen, B. B. Binary Colloidal Structures Assembled through Ising Interactions. *Nat. Commun.* **2012**, *3*, 794.
32. Junfeng, Z.; Lingjie, M.; Xinliang, F.; Xiaoke, Z.; Qinghua, L. One-Pot Synthesis of Highly Magnetically Sensitive Nanochains Coated with a Highly Cross-Linked and Biocompatible Polymer. *Angew. Chem., Int. Ed.* **2010**, *49*, 8476–8479.
33. Ye, M.; Zorba, S.; He, L.; Hu, Y.; Maxwell, R. T.; Farah, C.; Zhang, Q.; Yin, Y. Self-Assembly of Superparamagnetic Magnetite Particles into Peapod-Like Structures and their Application in Optical Modulation. *J. Mater. Chem.* **2010**, *20*, 7965–7969.
34. Hu, Y.; He, L.; Yin, Y. Magnetically Responsive Photonic Nanochains. *Angew. Chem., Int. Ed.* **2011**, *50*, 3747–3750.
35. Singh, H.; Laibinis, P. E.; Hatton, T. A. Rigid, Superparamagnetic Chains of Permanently Linked Beads Coated with Magnetic Nanoparticles. Synthesis and Rotational Dynamics under Applied Magnetic Fields. *Langmuir* **2005**, *21*, 11500–11509.
36. Sheparovych, R.; Sahoo, Y.; Motornov, M.; Wang, S. M.; Luo, H.; Prasad, P. N.; Sokolov, I.; Minko, S. Polyelectrolyte Stabilized Nanowires from Fe3O4 Nanoparticles via Magnetic Field induced Self-Assembly. *Chem. Mater.* **2006**, *18*, 591–593.
37. Amali, A. J.; Saravanan, P.; Rana, R. K. Tailored Anisotropic Magnetic Chain Structures Hierarchically Assembled from Magnetoresponsive and Fluorescent Components. *Angew. Chem., Int. Ed.* **2011**, *50*, 1318–1321.

38. Baudry, J.; Rouzeau, C.; Goubault, C.; Robic, C.; Cohen-Tannoudji, L.; Koenig, A.; Bertrand, E.; Bibette, J. Acceleration of the Recognition Rate between Grafted Ligands and Receptors with Magnetic Forces. *Proc. Natl. Acad. Sci. U.S. A.* **2006**, *103*, 16076–16078.
39. Promislow, J. H. E.; Gast, A. P.; Fermigier, M. Aggregation Kinetics of Paramagnetic Colloidal Particles. *J. Chem. Phys.* **1995**, *102*, 5492–5498.
40. Leal Calderon, F.; Stora, T.; Mondain Monval, O.; Poulin, P.; Bibette, J. Direct Measurement of Colloidal Forces. *Phys. Rev. Lett.* **1994**, *72*, 2959–2962.
41. Stiriba, S. E.; Kautz, H.; Frey, H. Hyperbranched Molecular Nanocapsules: Comparison of the Hyperbranched Architecture with the Perfect Linear Analogue. *J. Am. Chem. Soc.* **2002**, *124*, 9698–9699.
42. Lu, P. J.; Weitz, D. A. Colloidal Particles: Crystals, Glasses, and Gels. *Annu. Rev. Condens. Matter Phys.* **2013**, *4*, 217–233.
43. Lu, P. J.; Zaccarelli, E.; Ciulla, F.; Schofield, A. B.; Sciortino, F.; Weitz, D. A. Gelation of Particles with Short-Range Attraction. *Nature* **2008**, *453*, 499–503.
44. Sacanna, S.; Irvine, W. T. M.; Chaikin, P. M.; Pine, D. J. Lock and Key Colloids. *Nature* **2010**, *464*, 575–578.
45. Damasceno, P. F.; Engel, M.; Glotzer, S. C. Predictive Self-Assembly of Polyhedra into Complex Structures. *Science* **2012**, *337*, 453–457.
46. Chen, Q.; Bae, S. C.; Granick, S. Directed Self-Assembly of a Colloidal Kagome Lattice. *Nature* **2011**, *469*, 381–384.
47. Désert, A.; Hubert, C.; Fu, Z.; Moulet, L.; Majimel, J.; Barboteau, P.; Thill, A.; Lansalot, M.; Bourgeat-Lami, E.; Duguet, E.; Ravaine, S. Synthesis and Site-Specific Functionalization of Tetravalent, Hexavalent, and Dodecavalent Silica Particles. *Angew. Chem., Int. Ed.* **2013**, *52*, 11068–11072.
48. Kraft, D. J.; Ni, R.; Smallenburg, F.; Hermes, M.; Yoon, K.; Weitz, D. A.; van Blaaderen, A.; Groenewold, J.; Dijkstra, M.; Kegel, W. K. Surface Roughness Directed Self-Assembly of Patchy Particles into Colloidal Micelles. *Proc. Natl. Acad. Sci. U.S.A.* **2012**, *109*, 10787–10792.
49. Bishop, K. J. M.; Wilmer, C. E.; Soh, S.; Grzybowski, B. A. Nanoscale Forces and Their Uses in Self-Assembly. *Small* **2009**, *5*, 1600–1630.
50. Hiemenz, P. C.; Lodge, T. P. *Polymer Chemistry*; CRC Press Inc: Boca Raton, FL, 2007.
51. Fischer, V.; Bannwarth, M. B.; Jakob, G.; Landfester, K.; Muñoz-Espí, R. Luminescent and Magnetoresponsive Multifunctional Chalcogenide/Polymer Hybrid Nanoparticles. *J. Phys. Chem. C* **2013**, *117*, 5999–6005.
52. Herrmann, C.; Bannwarth, M. B.; Landfester, K.; Crespy, D. Re-Dispersible Anisotropic and Structured Nanoparticles: Formation and Their Subsequent Shape Change. *Macromol. Chem. Phys.* **2012**, *213*, 829–838.